

surements.

*Work supported by the National Science Foundation and the Advanced Research Projects Agency.

¹B. O. Seraphin and R. B. Hess, Phys. Rev. Letters **14**, 138 (1965).

²K. L. Shaklee, F. H. Pollak, and M. Cardona, Phys. Rev. Letters **15**, 883 (1965).

³W. J. Turner and W. E. Reese, Phys. Rev. **117**, 1003 (1960).

⁴M. L. Cohen and T. K. Bergstresser, Phys. Rev. **141**, 789 (1966).

⁵F. H. Pollak and M. Cardona, to be published.

⁶B. O. Seraphin, Proc. Phys. Soc. (London) **87**, 239 (1966).

⁷K. L. Shaklee, F. H. Pollak, and M. Cardona, to be published.

⁸B. O. Seraphin and N. Bottka, Phys. Rev. (to be published).

⁹H. Ehrenreich, J. Appl. Phys. **32**, 2155S (1961).

¹⁰C. A. Mead and W. G. Spitzer, Phys. Rev. Letters **11**, 358 (1963).

¹¹M. Cardona, J. Appl. Phys. **32**, 2151S (1961).

¹²T. E. Fischer, Phys. Rev. **139**, A1228 (1965).

¹³ $\Delta_0 = 0.75$ eV. See R. Braunstein, Bull. Am. Phys. Soc. **4**, 133 (1959).

¹⁴R. F. Blunt, H. P. R. Frederikse, J. H. Becker, and W. R. Hosler, Phys. Rev. **96**, 578 (1954).

¹⁵R. Zallen and W. Paul, Phys. Rev. **134**, A1628 (1965).

¹⁶J. C. Phillips and B. O. Seraphin, Phys. Rev. Letters **15**, 107 (1965).

¹⁷D. Aspnes, private communication; J. C. Phillips, to be published.

¹⁸M. Cardona, J. Phys. Chem. Solids **24**, 1543 (1963). Eq. (13) in this reference should read

$$M = -Q^2/[E_g(\Gamma_{15c}) - E_g(\Gamma_{15v})].$$

QUANTUM EFFECTS IN MICROWAVE HELICON PROPAGATION IN DEGENERATE SEMICONDUCTOR PLASMAS

Jacek Furdyna*

National Magnet Laboratory,† Massachusetts Institute of Technology, Cambridge, Massachusetts
(Received 10 February 1966)

In the usual formulation, the dispersion of helicon waves is independent of quantum contributions as well as of the form of the distribution function. Helicon absorption, on the other hand, is quite sensitive to both, and in the degenerate quantum limit should display oscillations of the Shubnikov-de Haas type. Such quantum phenomena have been experimentally observed under "local" conditions in metals by Grimes¹ and have also been considered theoretically for the "nonlocal" region in both semiconductors and metals by Quinn² and Miller.³ This Letter reports for the first time the observation and quantitative interpretation of very pronounced quantum oscillations in the damping of helicons propagating through highly degenerate semiconductor plasmas in the presence of quantizing magnetic fields. The observed oscillatory behavior of the helicon amplitude is accompanied by weak but measurable quantum oscillations in the phase of the transmitted helicon waves, possibly associated with variations of the carrier density. The experiments, carried out at liquid-helium temperatures on several highly degenerate samples of *n*-type InSb and InAs, were performed by transmitting circularly polarized microwaves at 35 Gc/sec in the presence of

magnetic fields up to 100 kG. At fields corresponding to the threshold of the "quantum limit," the effect of spin splitting of the first Landau level can be readily resolved in the InSb data. At fields exceeding the oscillatory region (i.e., in the "extreme quantum limit"⁴) damping out of the helicon amplitude is observed, in marked contrast with helicon behavior in other media.

For circularly polarized waves propagating along an applied dc magnetic field through a conductor characterized by a spherical constant-energy surface, the solutions of the wave equation $k_{\pm}^2 \equiv (\alpha_{\pm} + i\beta_{\pm})^2 = \omega^2 \mu_0 \epsilon_{\pm}$ are related to the conductivity tensor as follows:

$$\epsilon_{\pm}' = \epsilon_l + (\sigma_{xx}'' \pm \sigma_{xy}')/\omega, \quad (1)$$

$$\epsilon_{\pm}'' = (\sigma_{xx}' \mp \sigma_{xy}'')/\omega, \quad (2)$$

where k is the complex propagation constant, z the direction of the dc magnetic field B , ϵ_l the lattice dielectric constant, ω the angular frequency, and μ_0 the permeability of free space. Here the single and double primes denote real and imaginary parts, respectively, and the subscript (+) and (-) signs refer to the two senses of polarization. The helicon mode of

propagation corresponds to the (+) solution under the conditions $(\omega_p^2/\omega) \gg \omega_c \gg \omega$, τ^{-1} which leads to the inequalities $\sigma_{xy}' \gg \sigma_{xx}'$, σ_{xx}'' , $\sigma_{xx}' \gg \sigma_{xy}''$, and $\sigma_{xy}' \gg \omega\epsilon l$, where ω_p and ω_c are the plasma and cyclotron frequencies and τ is the effective relaxation time. Since in this Letter only the helicon mode will be considered, the (+) subscript will henceforth be dropped. It is easily shown that under the above conditions α and β , i.e., the dispersive and absorptive parts of k , respectively, become

$$\alpha = (\mu_0 \omega \sigma_{xy}')^{1/2}, \quad (3)$$

$$\beta = \frac{1}{2}(\mu_0 \omega / \sigma_{xy}')^{1/2} \sigma_{xx}'. \quad (4)$$

Equations (3) and (4) are valid for the local approximation, but are otherwise independent of the semiconductor model. The latter enters through the explicit form of the conductivity tensor itself. Under conditions describing the helicon approximation, particularly $\omega_c \gg \omega$, the tensor components appearing in Eqs. (3) and (4) are practically frequency independent, and may therefore be satisfactorily replaced by the corresponding dc expressions. Thus the behavior of α and β in the degenerate quantum region can be expressed in terms of the known dc properties of σ_{xx}' and σ_{xy}' corresponding to this region.⁴

In the strongly degenerate quantum region considered in this Letter, the inequalities $\zeta \gg kT$ (where ζ is the Fermi energy) and $\hbar\omega_c \gg kT$ are satisfied in addition to the condition $\omega_c \tau \gg 1$ implicit in the helicon approximation. It is well known for dc transport theory⁴ that even under these conditions σ_{xy}' will remain independent of quantum effects as long as the carrier density is conserved, while σ_{xx}' , which depends directly on carrier scattering, with display an oscillatory character. Thus, under conservation of total carrier density, the helicon dispersion will remain insensitive to quantum effects (except through small second-order contributions), while the transmitted helicon amplitude will oscillate strongly as a function of the applied magnetic field. The maxima in diagonal conductivity, and thus the minima in the transmitted helicon amplitude, correspond to the singularities in the density of states, i.e., to magnetic fields satisfying the condition⁵

$$\zeta = (N + \frac{1}{2})\hbar\omega_c + \frac{1}{2}S|g|\mu_B B, \quad (5)$$

where N is an integer, μ_B the Bohr magneton,

g the g factor for the conduction electrons, and S takes the values $+1$ and -1 for the two spin orientations. It must be remembered that ζ is itself magnetic-field dependent and that in materials with moderate carrier concentration this variation is exceedingly important in the high-field limit, i.e., where $\hbar\omega_c \approx \zeta$. It is easily seen from Ref. 5 that magnetic fields satisfying condition (5) are given by the expressions

$$B_N^+ = \frac{2\hbar}{e} \left\{ \frac{2}{\pi^2 n} \sum_{k=0}^N \left[k^{1/2} + \left(k + \frac{m^*}{m_{sp}} \right)^{1/2} \right] \right\}^{-2/3}, \quad (6)$$

$$B_N^- = \frac{2\hbar}{e} \left\{ \frac{2}{\pi^2 n} \sum_{k=1}^N \left[k^{1/2} + \left(k - \frac{m^*}{m_{sp}} \right)^{1/2} \right] \right\}^{-2/3}, \quad (7)$$

where Eqs. (6) and (7) correspond to the spin states $S=+1$ and -1 , respectively, and m_{sp} is the spin mass $2m_0/|g|$. The effect of the splitting of Landau levels on the helicon amplitude, if experimentally resolvable, provides a measure of the g factor, much as in dc magnetoresistance experiments.⁶ The position of the extremum B_0^+ corresponding to the last quantum oscillation also depends strongly on the value of the g factor.

Helicon wave transmission was investigated at 35 Gc/sec in a series of highly degenerate samples of n -type InSb and InAs with the concentration n ranging from 10^{16} to 10^{18} cm⁻³. Lower concentrations were not investigated to avoid complications arising from the proximity of the magnetoplasma edge and from carrier freeze-out. The experiments were performed at 4.2 and 1.5°K, in magnetic fields up to 100 kG, i.e., extending into the "quantum limit"⁴ in these materials. A Rayleigh-type interferometer bridge, described elsewhere,⁷ was used in the experiments with minor modifications adapting the arrangement to measurements at liquid-helium temperatures. The samples were thick compared to the skin depth to minimize amplitude distortion due to Fabry-Perot-type dimensional resonances. The sample holders were so constructed that microwave leakage around the sample was negligible compared with the transmitted helicon amplitude.

A typical transmission spectrum, obtained with an InSb sample of relatively low doping ($n=1.1 \times 10^{16}$ cm⁻³), is shown in Fig. 1. Curve A represents the magnetic-field dependence of the helicon amplitude at 4.2°K, observed for

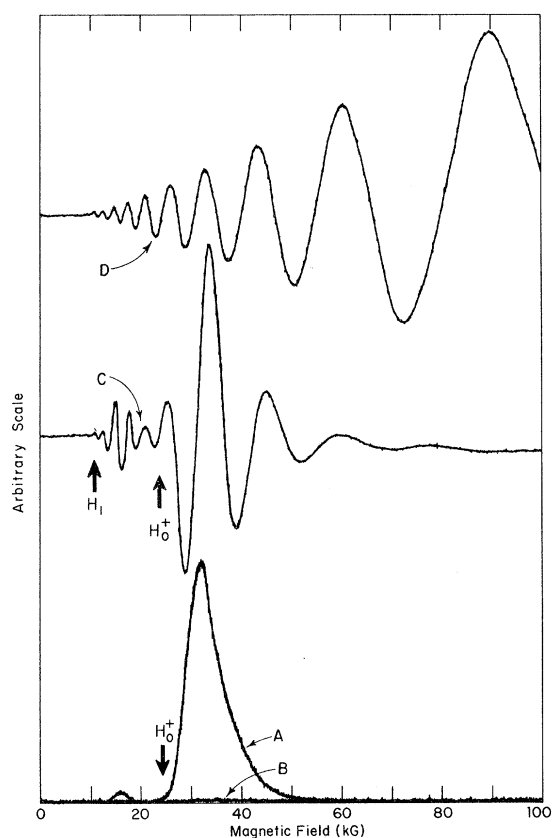


FIG. 1. X-Y recorder data showing transmission of circularly polarized microwaves versus magnetic field for *n*-type InSb with $n = 1.1 \times 10^{16} \text{ cm}^{-3}$. Curve A represents the magnetic-field dependence of the helicon amplitude at 4.2°K. Trace B, obtained under conditions similar to A with magnetic field reversed, illustrates the nonreciprocal nature of the helicon phenomenon. Curves C and D are Rayleigh interference patterns obtained, respectively, at 4.2 and 77°K. Note the striking contrast in the behavior of the helicon amplitudes (envelopes of the Rayleigh patterns) at the two temperatures, and, in particular, the vanishing of the helicon transmission at high fields in curve C. The arrow indicates the theoretical value of B_0^+ obtained via Eq. (6).

longitudinal propagation and incident circular polarization. Curve B is obtained under conditions corresponding to A, with reversed magnetic field, showing unambiguously the nonreciprocal nature of the phenomenon. Curves C and D are Rayleigh patterns showing interference between the transmitted helicon waves at 4.2 and 77°K, respectively, and a constant reference signal which considerably exceeds the helicon amplitude. Note that, while magnetic-field dependence of helicon dispersion does not depend markedly on temperature, the

difference in the amplitude behavior at the two temperatures is quite striking. A curve such as C provides simultaneously the measurement of concentration (obtained from the periodicity of the interference pattern on $B^{-1/2}$ scale) and the microwave Shubnikov-de Haas effect (obtained from the envelope of the interference pattern).

An integer plot of the phase variation at 4.2°K as a function of $B^{-1/2}$ does, in fact, show a weak but reproducible oscillation in the helicon dispersion, particularly at lower concentrations. No systematic analysis of this feature has as yet been carried out, but the initial calculations indicate that the effect cannot be entirely explained by the oscillatory higher order terms present in the complete dispersion relation. As recently suggested,⁸ it is possible that the carrier density itself varies appreciably at the threshold of the quantum limit. It should be mentioned that, since the contribution of higher order oscillatory terms to helicon phase variation and to the conventional Hall effect⁹ are different, the two quantities can be used simultaneously to eliminate this contribution and thus to isolate the actual variation of carrier concentration at high fields.

The positions of the observed amplitude minima corresponding to quantum numbers 1 to 4 (the latter observed in the most highly doped sample by the Rayleigh method) are in good agreement with the fields calculated via Eqs. (6) and (7), using the values of the effective mass¹⁰ and the *g* factor¹¹ for the respective carrier concentrations. The calculated fields are indicated by arrows in the figures. The observed field for the last singularity, B_0^+ , is systematically lower than that given by Eq. (6), as shown in Fig. 1. Recently the problem of the departure of B_0^+ from Eq. (6) was considered in connection with dc experiments.⁸ Although no rigorous theory is as yet available, it is shown that there exist several mechanisms, particularly carrier collisions and variation of carrier concentration in this region, which tend to lower the theoretical value of B_0^+ .

In the high-field limit, beyond the oscillatory region, Fig. 1 illustrates the damping out of the helicon waves at 4.2°K, in marked contrast with the higher temperature data and with helicon experiments involving other systems. This behavior is consistent with the magnetic-field dependence of diagonal conductivity in the "extreme quantum limit" in strongly degen-

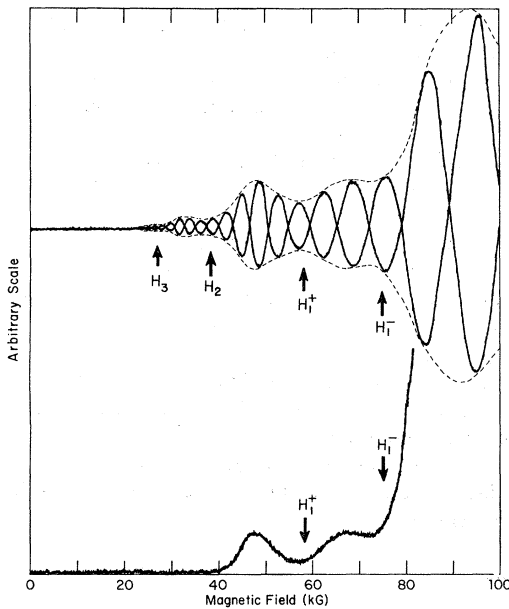


FIG. 2. Helicon transmission data versus magnetic field obtained with n -type InSb, $n = 1.6 \times 10^{17} \text{ cm}^{-3}$. The lower curve represents helicon amplitude. The upper curves are two Rayleigh interference patterns obtained at two phase-shifter settings 180° apart. The dashed line indicates the envelope obtained with these, and two other patterns phase shifted by 90° . Note the spin splitting of the first Landau level, clearly present in both sets of data.

erate plasmas characterized by dominant ionized impurity scattering,⁴ where σ_{xx} increases as B , leading to a $B^{3/2}$ variation of β . It is significant in this connection, as well as in connection with determining B_0^+ , that the function measured through β in the helicon experiment, $\sigma_{xx}\sigma_{xy}^{-1/2}$, differs in form from the conventional magnetoresistance, $\sigma_{xx}\sigma_{xy}^{-2}$, since the positions of the extrema, particularly B_0^+ and the last maximum, can be considerably shifted by the rapidly varying denominator.

Figure 2 illustrates the effect of spin splitting of the $N=1$ Landau level on the helicon amplitude transmitted through a sample with $n = 1.6 \times 10^{17} \text{ cm}^{-3}$. The calculated values of B_{1^+} and B_{1^-} , obtained via Eqs. (6) and (7) (indicated by the arrows), are in good agreement with the observed behavior. The effect of spin splitting was confirmed in samples with several doping levels. In general, care must be exercised in measuring structure of this type by helicon propagation, since multiple-reflection phenomena and leakage interference⁷ can produce features which are qualitatively com-

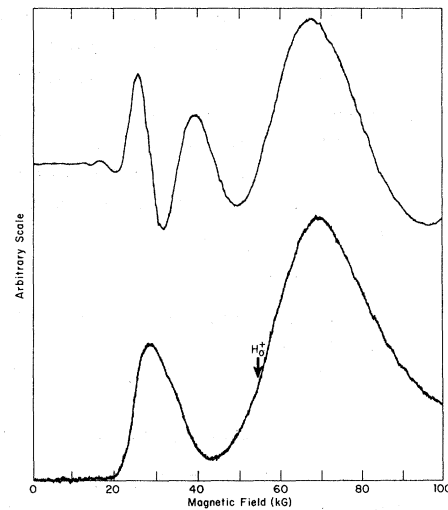


FIG. 3. Typical helicon amplitude and Rayleigh interference data versus magnetic field obtained for n -type InAs, $n = 2.5 \times 10^{16} \text{ cm}^{-3}$. Note the qualitative similarity to the behavior observed for degenerate InSb. The sharpness of the quantum oscillations, lower than in InSb, increases slightly as the temperature is decreased. The theoretical field corresponding to the last quantum oscillation, obtained using $g = 16$, exceeds the last minimum even more than in the case of InSb.

parable. Such errors of geometric nature have been ruled out in the present investigation by repeating the measurements on several samples of varying thickness.

Similar measurements were carried out on samples of n -type InAs. Figure 3 shows typical transmission data obtained on an InAs sample with $n = 2.5 \times 10^{16} \text{ cm}^{-3}$. The observed B_0^+ occurs even lower relative to the calculated values than in the case of InSb. The position of B_{1^+} , observed clearly in another sample of higher doping, is in satisfactory agreement with the calculated field. Spin splitting was not resolved in the InAs experiments. The dispersion in InAs displays an oscillation which in the preliminary data appears to be somewhat more pronounced than in InSb. High-field helicon damping is again observed beyond the oscillatory region.

Preliminary experiments have shown similar effects in HgTe and HgSe. A further experiment investigation of these effects and a detailed quantitative analysis of the data, particularly the weak oscillation of helicon dispersion, the shift of B_0^+ , and the amplitude saturation at high fields, are in progress and will be presented in full in a future publication.

The author is grateful to Joshua Zak, Rolf Arndt, Lawrence G. Rubin, and Wlodek Zawadzki for suggestions and stimulating discussions; to Alan J. Strauss and Ronald J. Sladek for some of the samples used in this investigation; and to Paul Coluccio for his highly skilled assistance in constructing the apparatus and in carrying out the measurements.

*Present address: Physics Department, Purdue University, Lafayette, Indiana.

†Supported by the U. S. Air Force Office of Scientific Research.

¹C. C. Grimes, *Plasma Effects in Solids* (Dunod, Paris, 1965), p. 87.

²J. J. Quinn, *Phys. Letters* **7**, 235 (1963).

³P. B. Miller, *Phys. Rev. Letters* **11**, 537 (1963).

⁴E. N. Adams and T. D. Holstein, *J. Phys. Chem. Solids* **10**, 254 (1959).

⁵L. É. Gurevich and A. L. Efros, *Zh. Eksperim. i Teor. Fiz.* **43**, 561 (1962) [translation: *Soviet Phys.-JETP* **16**, 402 (1963)].

⁶Kh. I. Amirkhanov and R. I. Bashirov, *Zh. Eksperim. i Teor. Fiz.-Pis'ma Redakt.* **1**, 49 (1965) [translation: *JETP Letters* **1**, 49 (1965)].

⁷J. K. Furdyna, to be published.

⁸S. T. Pavlov, R. V. Parfen'ev, Yu. A. Firsov, and S. S. Shalyt, *Zh. Eksperim. i Teor. Fiz.* **48**, 1565 (1965) [translation: *Soviet Phys.-JETP* **21**, 1049 (1965)].

⁹These higher order contributions are obtained by retaining terms of order $\sigma_{xx}^2/\sigma_{xy}^2$ in the expansion of the parameters involved.

¹⁰J. Kolodziejczak, *Acta Phys. Polon.* **20**, 379 (1961).

¹¹L. M. Roth, B. Lax, and S. Zwerdling, *Phys. Rev.* **114**, 90 (1959).

MAGNETOSTRICTION CONSTANTS OF THE RARE-EARTH GARNETS FROM THE PRESSURE DEPENDENCE OF ELECTRON-PARAMAGNETIC-RESONANCE SPECTRA*

T. G. Phillips† and R. L. White

Stanford Electronics Laboratories, Stanford University, Stanford, California

(Received 7 March 1966)

We wish to report a technique for determining the single-ion contribution to the magnetoelastic constants of magnetic insulators, with particular reference to the contribution of Gd^{3+} to the magnetostriction constants of gadolinium iron garnet (GdIG). We proceed by relating the macroscopic magnetoelastic constants of the crystal to the microscopic magnetoelastic constants of the constituent ions, and then determining the relevant microscopic constants from the variation of the EPR spectra of the ions under uniaxial pressure.

The linear magnetostriction of ferromagnetic or ferrimagnetic crystals arises from the strain dependence of the magnetic anisotropy. For a cubic crystal, the magnetoelastic energy is usually written¹

$$E_{ME} = \sum_{ijkl} F_{ijkl}^{\text{cubic}} \epsilon_{ij} \alpha_k \alpha_l$$

$$= B_1 [(\alpha_1^2 - \frac{1}{3}) \epsilon_{xx} + (\alpha_2^2 - \frac{1}{3}) \epsilon_{yy} + (\alpha_3^2 - \frac{1}{3}) \epsilon_{zz}]$$

$$+ B_2 [\alpha_1 \alpha_2 \epsilon_{xy} + \alpha_2 \alpha_3 \epsilon_{yz} + \alpha_3 \alpha_1 \epsilon_{zx}]. \quad (1)$$

We note first that the cubic magnetoelastic tensor F_{ijkl}^{cubic} has only two independent constants,

B_1 and B_2 , closely related to the magnetostriction constants λ_{100} and λ_{111} . We note secondly that the magnetoelastic tensor involves terms quadratic in the spin coordinates (the direction cosines of the magnetization) rather than biquadratic in the spin coordinates as is the case for the magnetic anisotropy. It therefore follows that effects involving energies quadratic in the spin coordinates (required by symmetry to cancel out in first order in the total anisotropy energy) will dominate the magnetoelastic energy, and that the success of the single-ion model of magnetic anisotropy²⁻⁴ in the magnetic insulators does not imply the success of a single-ion model of magnetoelastic effects.

In the (cubic) rare-earth garnets, the rare-earth ions occupy six magnetically inequivalent sites each of orthorhombic symmetry. For the S-state ion Gd^{3+} , we write the magnetic Hamiltonian

$$\mathcal{H}_M = \sum_{\sigma} g \beta \vec{S}^{\sigma} \cdot \vec{H}_{\text{eff}} + \sum_{\sigma} \vec{S}^{\sigma} \cdot D^{\sigma} \cdot \vec{S}^{\sigma} + \text{terms in } S^4, S^6$$

$$+ \text{terms involving more than one ion}, \quad (2)$$

where the summation in σ is over the six inequivalent sites. For the iron garnets, \vec{H}_{eff} will be the molecular field arising from the